THE BICIRCULAR MODEL NEAR THE TRIANGULAR LIBRATION POINTS OF THE RTBP

Carles Simó,[1] Gerard Gómez,[1] Àngel Jorba, [2] and Josep Masdemont [2]

[1]Departament de Matemàtica Aplicada i Anàlisi
Universitat de Barcelona
Gran Via 585, 08007 Barcelona (Spain)
[2]Departament de Matemàtica Aplicada I
Universitat Politècnica de Catalunya
Diagonal 647, 08028 Barcelona (Spain)

Abstract

We present a study of a simplified model of the Restricted Four Body Problem consisting of Earth, Moon, Sun and a massless particle, as a model of the dynamics of a spacecraft. The region where we look for the motion is a vicinity of the triangular libration points of the Restricted Three Body Problem. The model we discuss here is the so called Bicircular Problem. The main question is the existence of zones where the motion has good stability properties. The answer is positive, but the stable motions can not be confined to a small distance of the ecliptic plane. Both numerical simulations and analytical results are presented. Some tentative explanations offer a possible way to study many other kinds of problems. Some applications to space missions are mentioned.

INTRODUCTION

The objective of the work is to understand the kinds of motion which appear on a vicinity (may be a large vicinity) of the geometrically defined equilateral points of the Earth-Moon system when the bicircular model is considered. In this Introduction we summarize the present knowledge, some of the achievements of this work and we discuss the main difficulties of the problem.

The simplest model for the motion near the triangular libration points is, of course, the spatial Restricted Three Body Problem (RTBP). With respect to the RTBP the main perturbations are due to the presence of the Sun as it is shown in Gómez et al.[5]. This is the reason to devote our attention to the bicircular problem.

From Newton to Chaos, Edited by A.E. Roy
and B.A. Steves, Plenum Press, New York, 1995

Definition of the model and equations of motion

The bicircular problem is a simplified version of a restricted four body problem. The objective is to describe the motion of a massless particle under the gravitational atraction of Earth, Moon and Sun. In this model we suppose that the Earth and the Moon are revolving in circular orbits around their centre of mass, B, and the Earth-Moon barycentre is moving in a circular orbit around the centre of masses of the Sun-Earth-Moon system. We remark that, with these assumptions, the motion of these three bodies is not coherent. That is, the assumed motions do not satisfy Newton's equations. However the model is extremely useful for some kind of orbits.

Let μ be the mass of the Moon, $1-\mu$ the mass of the Earth and m_S the mass of the Sun. Let the distance from the Earth to the Moon be taken as unity. Then the distance from B to the Sun is a_S. We use synodic coordinates with respect to the Earth-Moon system, so that the positions of Earth and Moon are fixed at $(\mu,0,0)$ and $(\mu-1,0,0)$, respectively. The mean angular velocity of the Sun in these synodic coordinates is denoted by ω_S.

To keep a Hamiltonian form we use synodic coordinates x, y, z, for the position of the massless body, but instead of the velocities we use momenta p_x, p_y, p_z, defined by $p_x = \dot{x} - y$, $p_y = \dot{y} + x$, $p_z = \dot{z}$.

In this way the equations of the bicircular problem are:

$$\begin{aligned}
\dot{x} &= p_x + y,\\
\dot{y} &= p_y - x,\\
\dot{z} &= p_z,\\
\dot{p}_x &= p_y - \frac{1-\mu}{r_{PE}^3}(x-\mu) - \frac{\mu}{r_{PM}^3}(x-\mu+1) - \frac{m_S}{r_{PS}^3}(x-x_S) - \varepsilon_S\cos\theta,\\
\dot{p}_y &= -p_x - \left(\frac{1-\mu}{r_{PE}^3} + \frac{\mu}{r_{PM}^3}\right) y - \frac{m_S}{r_{PS}^3}(y-y_S) + \varepsilon_S\cos\theta,\\
\dot{p}_z &= -\left(\frac{1-\mu}{r_{PE}^3} + \frac{\mu}{r_{PM}^3} + \frac{m_S}{r_{PS}^3}\right) z,
\end{aligned}$$

where $r_{PE}^2 = (x-\mu)^2 + y^2 + z^2$, $r_{PM}^2 = (x-\mu+1)^2 + y^2 + z^2$ and $r_{PS}^2 = (x-x_S)^2 + (y-y_S)^2 + z^2$, with $x_S = a_S\cos\theta$, $y_S = -a_S\sin\theta$, $\theta = \omega_S t + \theta_0$, and θ_0 is some initial phase of the Sun. For shortness we have used the perturbation parameter of the Sun $\varepsilon_S = \frac{m_S}{a_S^2}$.

For further use we give here the related Hamiltonian

$$H = \frac{1}{2}(p_x^2 + p_y^2 + p_z^2) + yp_x - xp_y - \frac{1-\mu}{r_{PE}} - \frac{\mu}{r_{PM}} - \frac{m_S}{r_{PS}} - \frac{m_S}{a_S^2}(y\sin\theta - x\cos\theta).$$

The values of the parameters that we have used for the symbolic and numerical computations are as follows:
Mass parameter for the Earth-Moon system:

$$\mu = \frac{1}{82.300587} \approx 0.012150582.$$

Sun mass (1 unit = Earth+Moon mass):

$$m_S = \frac{0.29591220828559 \times 10^{-3}}{0.89970116585573 \times 10^{-9}}.$$

Mean angular velocity of the Sun in synodic coordinates:

$$\omega_S = 1 - \frac{129602770.31}{1732564371.15}.$$

Semimajor axis of the Sun (1 unit = Earth-Moon distance):

$$a_S = \left(\frac{1+m_S}{(1-\omega_S)^2}\right)^{1/3}.$$

Known results near $L_{4,5}$

The bicircular problem can be obtained from the circular RTBP by continuation with respect to the mass of the Sun or by means of some intermediate Hill's problem (see Gómez et al.[4] and references therein).

There are three simple periodic orbits (two of them linearly stable and another one small and slightly unstable) with period equal to the synodic period of the Sun in the Earth-Moon system: $T_S = 6.79117$. The two stable orbits lie relatively far away from the triangular libration points of the RTBP and, when the full set of perturbations is included, they become slightly unstable (see Gómez et al.[4]). One can use a continuation method to pass from the RTBP to the bicircular model by introducing a parameter ε instead of ε_S in the equations, and then by increasing it from zero to ε_S. At the zero value we can take the L_5 point (or, equivalently, the L_4 one) as initial condition. Of course, it can be considered as a T_S periodic orbit. For small values of ε a periodic orbit is obtained, close to a small loop travelled twice around L_5. By increasing ε till ε_S, the orbit we reach is one of the big periodic orbits mentioned above. The other big orbit is essentially identical but with a change in the phase. Starting at this orbit and decreasing now ε, a turning point is found. When crossing the turning point, the stability of the periodic orbit along the family changes. From that point on ε increases again, and when it reaches the value ε_S the small unstable periodic orbit is obtained. The characteristic curve can be seen as obtained from a pitchfork by symmetry breaking. From now on we shall consider these small periodic orbits as the substitute of the triangular libration points in the case of the bicircular model, despite they can not be obtained by direct continuation (see Figure 1).

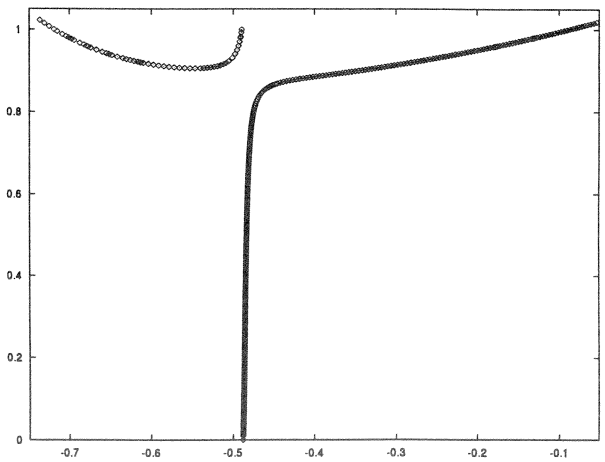

Figure 1

We remark that for other natural 4-body problems in the Solar System, where the bicircular model can be used as an approximation near some triangular points of a RTBP, the behaviour can be different. For instance, consider as RTBP the system Sun-Jupiter-asteroid and take Saturn as fourth body. In a bicircular model one finds that, under the influence of Saturn, the L_4 and L_5 points are replaced by small stable periodic orbits. The same is true if we consider the L_4, L_5 points of the Sun-Saturn system when perturbed by Jupiter.

No fixed points, nor autonomous first integral exist for the bicircular problem. The existence of a "stable domain" in some extended vicinity of the small periodic orbit is, up to here, an open question. We will see later on that, according to our numerical simulations, these stable domains exist. In fact similar domains, with good stability properties, exist also for the full problem (i.e., when all the solar system is taken into account) and are close to the ones found for the bicircular model (see Gómez et al.[5]).

Main difficulties of the problem

We can summarize the difficulties to be found in our problem after the previous results are known:

1. An external frequency appears together with the (amplitude varying) inner frequencies. These 4 frequencies lead to many resonances.

2. The effect of the Sun is uniformly large in the vicinity of $L_{4,5}$.

3. At the geometrical $L_{4,5}$ the frequencies of: the proper short period, the vertical oscillations and the synodic frequency of the Sun are rather close.

In the circular RTBP we are faced to a three degrees of freedom autonomous Hamiltonian. In the bicircular case the system is periodic instead of autonomous. Even in the 3-D autonomous case, to describe to some extent the dynamical behaviour in big regions of the phase space can be a formidable task.

Starting at some integrable problem and adding a perturbation with increasing parameter we find, successively:

a) For the integrable problem the phase space is completely foliated by invariant manifolds, mainly 3-D tori.

b) For small perturbations (or, equivalently, when we look very close to a totally elliptic equilibrium point) most of the 3-D tori subsist, as assured by the celebrated KAM theorem (see Arnol'd and Avez[1]), and very small zones of chaotic motion appear. They are hardly seen in practice if the perturbation is small because of the exponentially small character of the splitting of separatrices (see Lazutkin et al.[7], Fontich and Simó[2], Simó[9]. As the 3-D tori do not separate the levels of energy (which are 5-dimensional), Arnol'd diffusion can appear as a wandering motion between the tori. This prevents, in general, the existence of true barriers for the motion of the momenta. However, this motion is, at most, extremely slow, as assured by the results of Nekhorosev[8].

c) When the perturbation is increased (or, equivalently, when we look at a relatively large distance from a totally elliptic equilibrium point), the 3-D tori are destroyed by some not yet fully understood mechanism. However, cantorian families of normally hyperbolic tori still subsist. They constitute a kind of skeleton of the

motion. In some sense, one can consider the motion as a sequence of passages near lower dimensional tori, where they stay for some time interval before reaching the vicinity of next tori, following closely a heteroclinic orbit. The observed behaviour in the Solar System simulations for very long time intervals seems to be of this type (see Laskar[6]).

In the present case we have, as an additional difficulty, the fact that the system is not autonomous but periodic. In principle, we can assume that the system is reduced to autonomous form by means of time-dependent canonical changes. But this is purely formal and, furthermore, we can be faced to resonances in this process. If no resonances appear and we are satisfied with a study for moderate time intervals, we can describe the motion as the one of the autonomous system obtained after the canonical changes, which is then shaken by the periodic change of variables.

Contents of the work

In the second Section we describe numerical simulations carried out for the bicircular model. We present the results concerning sets of points which subsist, in an extended neighbourhood of the former triangular equilibrium points, for a long time span. Furthermore frequency analysis of several orbits have been carried out. The Section is ended with a discussion of the results. These ones suggest some reasonable explanations. Just looking at the frequency analysis we can detect the key role played by the inner frequencies on the system (that is, what can be seen as a generalization of the vertical, short period and long period modes of the circular RTBP), together with the solar synodic frequency. A sketch of the geometrical and analytical explanations of the zone of stable motion is presented.

The third Section describes the reduction of the bicircular model to some Normal Form. The essential part is to convert the periodically dependent Hamiltonian in an autonomous one. This is done around the small unstable periodic orbit described above. Then one obtains a clear explanation for the instability found in the numerical simulations of that problem for small values of the z amplitude. The source of the instability is the 1-1 resonance between the short period frequency and the solar one. An analytical description and some illustrations are given for the 2-D unstable tori which emerge from the small unstable periodic orbit when the vertical mode is added.

The work is ended with some discussion and conclusions concerning the applicability of the results to space missions.

NUMERICAL SIMULATIONS

Description of the massive simulations

A typical computation, for the determination of the stability zones, starts as follows. Give values ρ, α, z. Then select a point x, y, z by $x = (1+\rho)\cos(2\pi\alpha) + \mu$, $y = (1+\rho)\sin(2\pi\alpha)$. We shall use α between zero and $1/2$. So we are doing the computations near the position of L_5 in the RTBP, the case of L_4 being symmetric. Take zero initial velocity in synodic coordinates ($\dot{x} = \dot{y} = \dot{z} = 0$). Perform an integration for a time span up to some prescribed t_f. Stop the computation if $y < 0$ at some value of t, $t \leq t_f$. If we reach t_f the position (ρ, α, z) is stored as belonging to the "stable domain" in some weak sense.

In the bicircular problem the triangular libration points do not longer exist. In its place there are unstable periodic orbits (see Introduction, Gómez et al.[4,5]). So, locally near that orbit, the points escape. As the system is not autonomous, we have to take into account the initial phase of the Sun, θ_0. This initial phase plays an important role in the stable domain. The effect is almost the same when the initial phase in increased by π. To see the effect for different initial phases of the Sun we refer to Gómez et al.[5]. Here, for shortness we consider $\theta_0 = 0$ in all the simulations.

At this moment some considerations must be done. They apply to the bicircular problem, but are also valid for the RTBP, both in the circular and the elliptic cases. The first one concerns the set of initial data. Taking zero initial (synodic) velocity seems to be a strong restriction. Consider, however, the case of a totally elliptic fixed point of a Hamiltonian system, and assume that the frequencies are rationally independent. In a small vicinity of that point the motion takes place mainly on tori. Let q_j and p_j denote some local coordinates, reducing the quadratic part of the Hamiltonian to diagonal form. The motion is close to $q_j = A_j \cos(\omega_j t + \phi_j)$, $p_j = -A_j \omega_j \sin(\omega_j t + \phi_j)$, for some frequencies, ω_j, and phases ϕ_j. Assume p_j are the velocities (otherwise, it is similar). By the density of the orbits in the tori, there exists some time such that all the velocities are so close to zero as desired. It is true that, if at some distance of the fixed point there is a linearly stable periodic orbit, surrounded by some tori, the motion on them is stable and the velocity on these tori is never zero. Another consideration is that, if most of the motion takes place on tori (or close to them), taking an initial generic 3-D set (as it seems to be the set with zero synodic velocity) the flow will span a 6-D domain.

The second consideration concerns the stability criterion. To choose $y < 0$ as an indicator of instability seems reasonable. It has been seen that, as soon as the orbit enters in that region, a wild behaviour shows up. Either passages near collision with the Earth or the Moon occur, or the motion is confined for some time near the region of the other triangular point, with an eventual escape of the vicinity of the Earth-Moon system. The criterion can be too strict for orbits reaching big values of z (say, larger than 0.8). May be orbits showing good stability properties (they seem to be in tori passing close to the L_5 point, in the position coordinates) and oscillate up and down, enter the $y < 0$ region near the extreme values of z. In any case this seems to affect only a small fraction of the initial conditions. The next question deals with the value of t_f. Usually points which escape, according to our criterion, go away in a relatively short time (say, 100 lunar periods). On the other hand, among the points subsisting for 10000 periods the escape takes place at a small rate. See the next subsections for more qualitative and quantitative information, and for the behaviour of the escaping rate.

The integrations have been carried out using an RKF78 method with automatic stepsize control and maximum local error equal to 10^{-13}.

Results of the simulations

For values of z ranging from 0 to 1 with step 0.05, we have taken values of ρ, α in the ranges [-0.250,0.025], [0.100,0.450], respectively, with stepsize 0.001 in both directions. The final time has been set to $t_f = 10000 \times 2\pi$, and all the points subsisting up to a time at least equal to $100 \times 2\pi$ have been recorded. The Table 1 presents a summary of results.

The Figure 2 displays the results for values of z equal to 0.25, 0.35, ..., 0.85 from top to bottom. The stable region after 10000 lunar synodic revolutions is shown. The

Table 1. Points which subsist after 10000 revolutions of the Moon for the bicircular problem. In the first row the value of z is given. From the second to the last row we display, respectively: Points subsisting for 100, 1000 and 10000 lunar revolutions, minima and maxima of $1000 \times \alpha$ and $1000 \times \rho$ for the points which subsist for 10000 revolutions. In all cases we have taken $\theta_0 = 0$.

.00	.05	.10	.15	.20	.25	.30	.35	.40
74	69	75	58	80	252	538	1189	2214
15	13	11	8	12	153	397	820	1537
12	10	9	5	2	139	381	720	1225
333	333	334	334	336	323	312	302	290
339	338	339	340	337	350	358	365	377
-3	-3	-5	-7	-12	-20	-28	-38	-50
-1	-2	-4	-6	-12	-14	-18	-22	-27
.45	.50	.55	.60	.65	.70	.75	.80	.85
2371	3214	3158	2630	2258	2099	1548	743	787
1484	1588	2224	1391	824	690	627	163	205
1279	1062	1748	847	366	228	397	69	115
295	283	290	289	313	323	310	331	328
376	371	378	372	366	373	360	346	348
-63	-74	-87	-98	-108	-122	-138	-162	-175
-37	-45	-50	-65	-82	-99	-123	-151	-166

horizontal variable is α and the vertical one is ρ. For α we have taken a range going from $\alpha = 0.38$ (to the left) to $\alpha = 0.285$ (to the right). The windows for ρ depend on z but all the ranges in ρ have amplitude equal to 0.04. The lower values of ρ in the windows are -0.035, -0.050, -0.070, -0.088, -0.115, -0.150 and -0.190, respectively. The divisions inside each plot correspond to multiples of 0.025, both in ρ and α.

The behaviour is quite different from the one found for the circular and elliptic RTBP (see Gómez et al.[5]). For z less than 0.25, almost all points disappear after 10000 revolutions. But from $z = 0.25$ till $z = 0.55$ the size of the stable region increases, to decrease again when higher values of z are taken. For some values of θ_0 some points subsist even for $z = 0.95$. Averaging over θ_0, the number of subsisting points for $z = 0.40, \ldots, 0.60$ is comparable to the RTBP case (compare Gómez et al.[5]).

Let us present an explanation for the stable points found till now. At L_5 point the RTBP, considering the Hamiltonian up to second degree, behaves like three harmonic oscillators. One of them, with frequency equal to 1, corresponds to vertical oscillations. When the full system is considered, these vertical oscillations give rise to a family of "vertical" periodic orbits. These orbits, in fact, project on the (x, y) plane close to an ellipse travelled twice and, on the (x, z) and (y, z) planes, as figure eight curves. The initial conditions can be chosen with $z = 0$. In the bicircular model, L_5 has been replaced by the small periodic orbit. In a similar way, the RTBP "vertical" periodic orbits are replaced by 2-D tori, unstable for small vertical amplitudes (see next Section). It seems that for larger z these 2-D tori become linearly stable. One can also consider them as a periodic perturbation of "big" orbits of the vertical family of the RTBP. Hence, motion near these 2-D stable tori must be, for a set of points of (big) positive measure on 4-D tori. Some of those points can sit on the 4-D manifold of zero synodical velocity (now we have 7 dimensions: 6 spatial and the time).

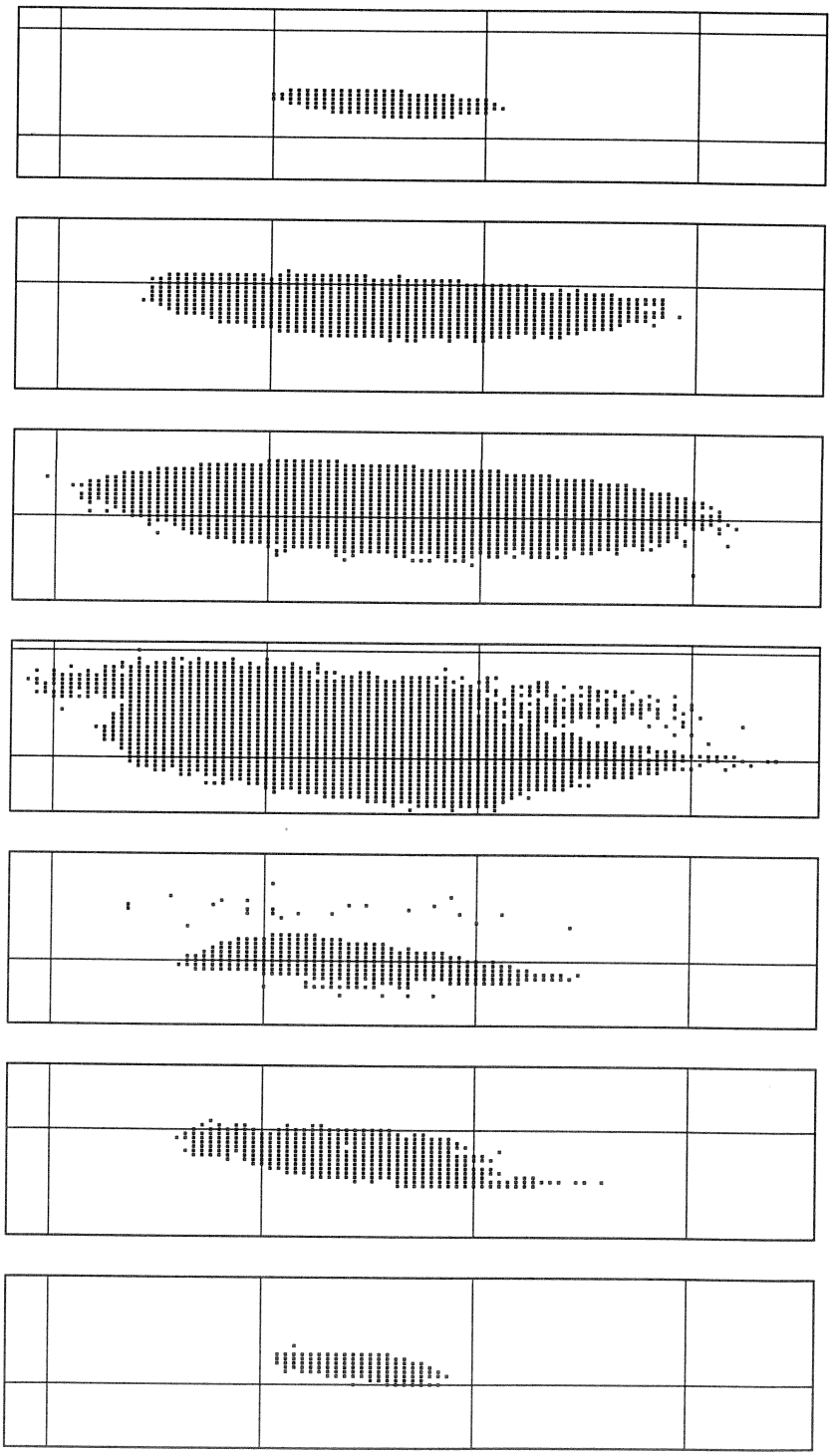

Figure 2. Representation of the stable region for several values of z. See the text for the concrete values and windows.

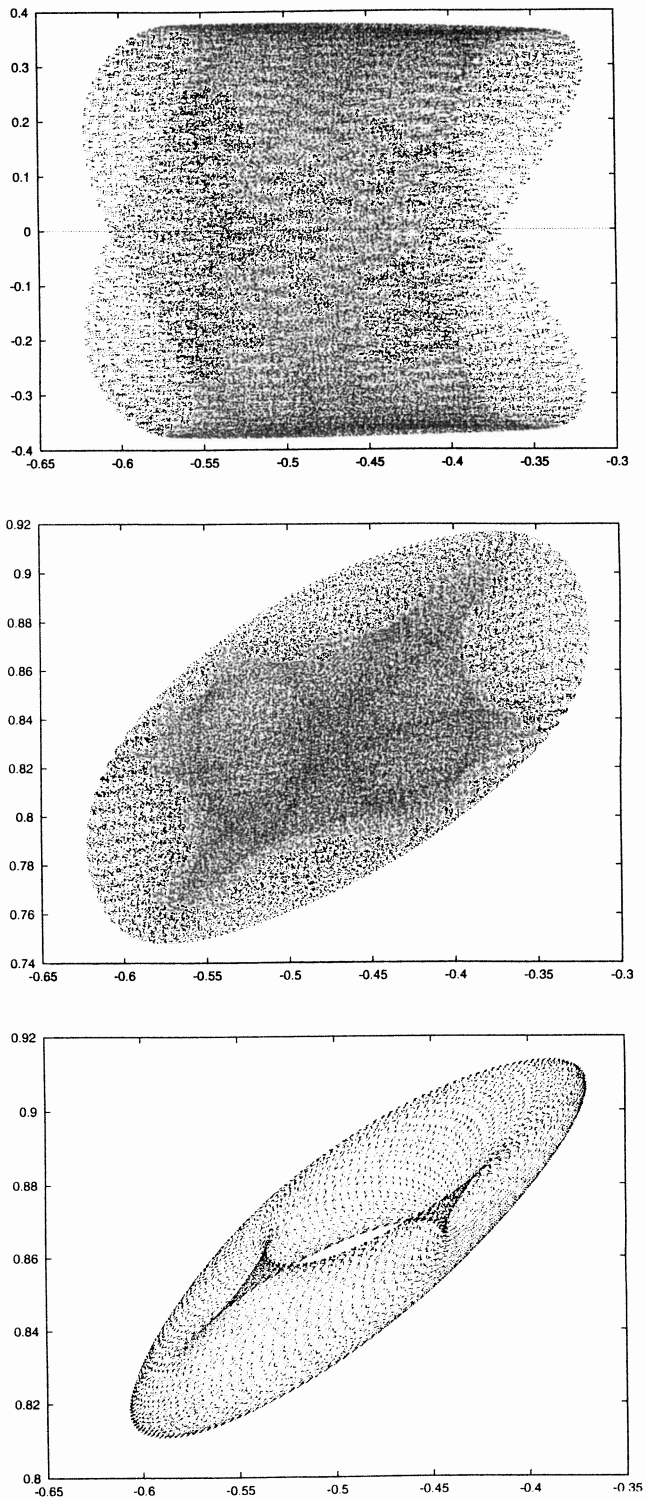

Figure 3. Projections of 3-D and 2-D tori for $\dot{z}_0 = 0.36$. See the text for additional explanation.

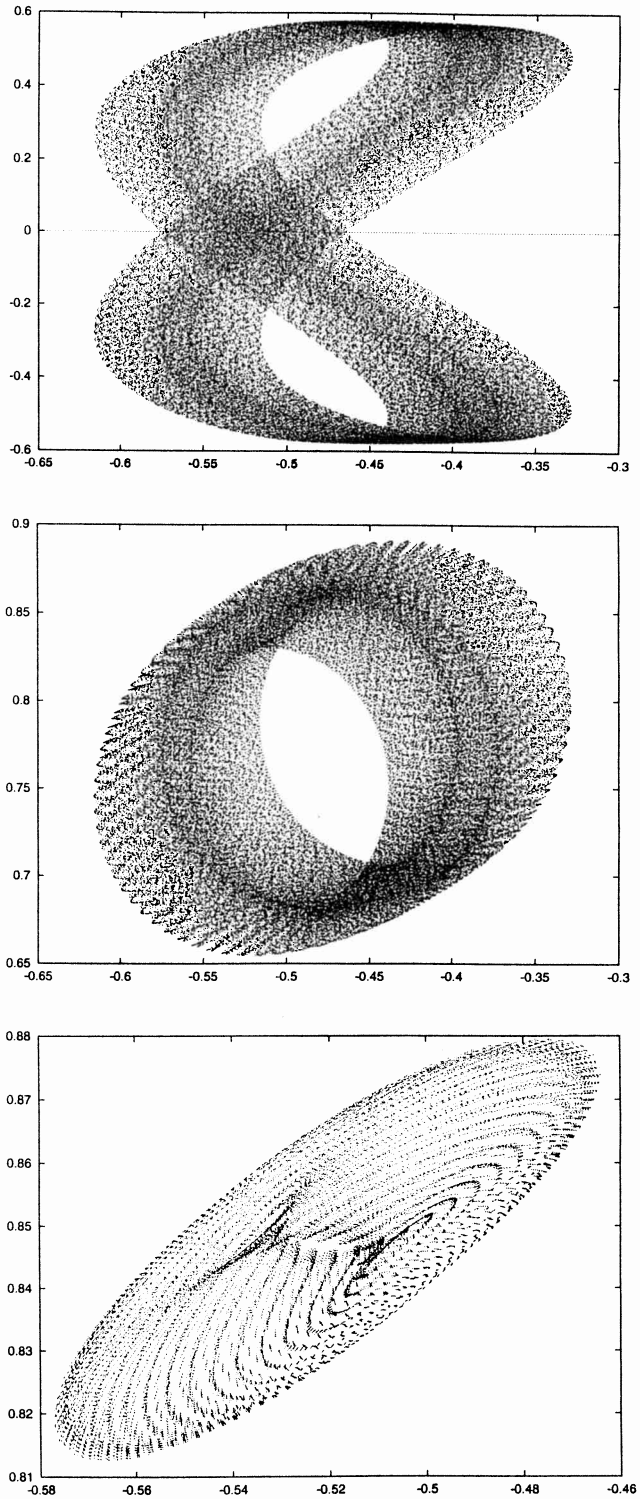

Figure 4. Projections of 3-D and 2-D tori for $\dot{z}_0 = 0.56$. See the text for additional explanation.

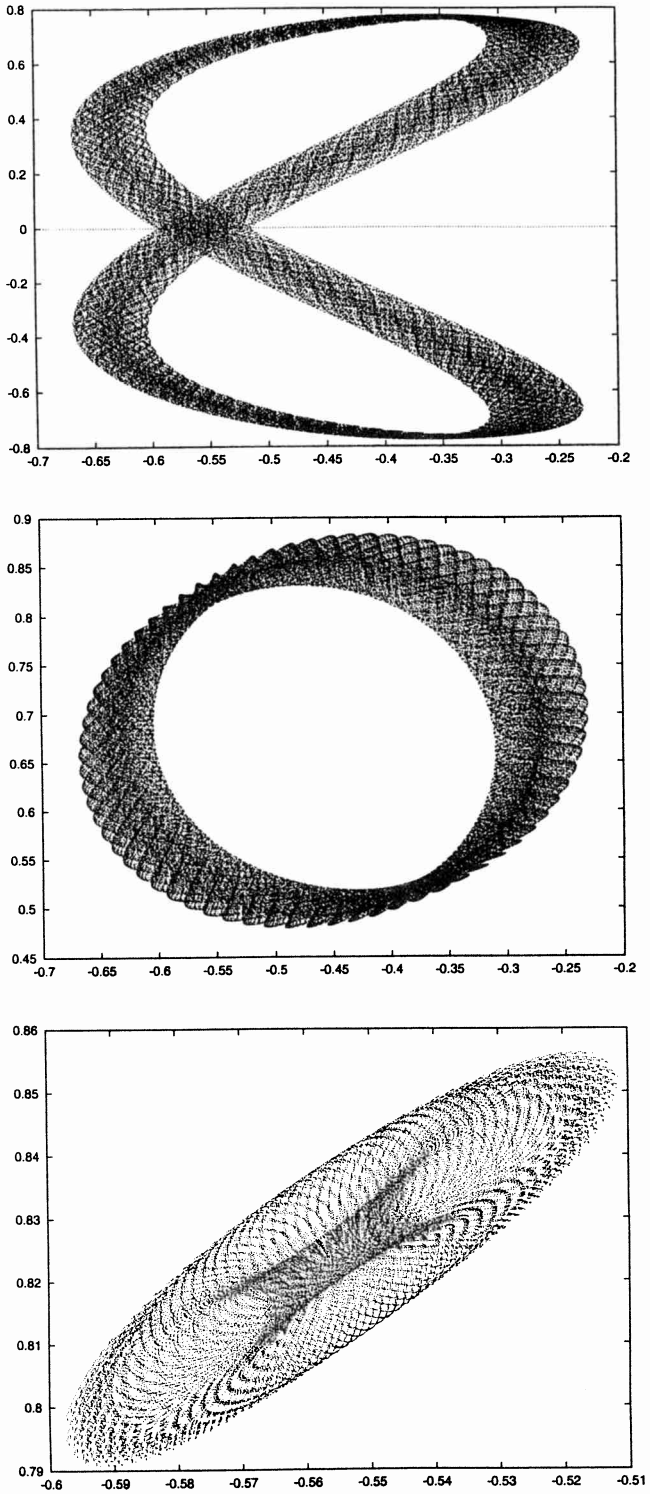

Figure 5. Projections of 3-D and 2-D tori for $\dot{z}_0 = 0.76$. See the text for additional explanation.

Some simulations with non zero initial synodic velocity

We can try another kind of simulations. Assume that we take as initial conditions the ones of the vertical family of periodic orbits of the RTBP, with $z = 0$ at $t = 0$ and also with zero initial phase of the Sun. We shall use as label for the orbit the initial value, $\dot{z}_0$, of $\dot{z}$ (this value is close to the maximum z-amplitude of the periodic orbit). For small z-amplitudes they must behave in an unstable way, but for larger amplitudes they can be stable, and even in some 4-D torus, typically, because of the preceding reasoning. We have tested this approach. To simplify the visualization we have used the "time the synodic period of the Sun"-map, to be denoted by T_{SS}. This is a 6-D canonical map and the invariant tori of maximal dimension, if any, must be 3-D. Even the 2-D projections of these 3-D tori can be difficult to recognize. To make things simpler one can take "slices" of the 3-D tori. The slices are defined by $|z| < 0.01 \times \dot{z}_0$. They should be close to 2-D tori, and their 2-D projections can be better identified as corresponding to 2-D tori.

The Figures 3,4 and 5 present the (x, z) and (x, y) projections of the 3-D tori and the (x, y) projection of the slice, from top to bottom. The values of $\dot{z}_0$ are taken equal to 0.36, 0.56 and 0.76, respectively. They have been chosen to have a representative sample (and, may be, by subjective aesthetic reasons). In all cases 4×10^6 iterates of T_{SS} have been done. The projections of the 3-D tori show only the 10^5 first iterates. For the slices we have considered all the iterates satisfying the slice condition. The respective number of points in the slices displayed are 24979, 25298 and 25792. To get a better feeling about the behaviour of the dynamics on the 3-D tori, one can look at how they appear on a computer screen when displayed at several rates of points/second. This is difficult to transmit in written form, so that we encourage the reader to try by himself. One can see that the points on the (x, z) projection travel along the "figure eight" shape of the set (this is very clear for $\dot{z}_0 = 0.76$) and the amplitudes behave in a pulsating way. These facts give a good evidence that the points sit in 3-D tori.

Frequency analysis

One can perform a frequency analysis of the x, y and z coordinates, as functions of time, for the orbits with initial conditions the ones of the vertical periodic orbits of the RTBP and zero initial phase of the Sun, as before. A refined Fourier analysis allows for a precise determination of the basic frequencies (see Gómez et al.[5]). The method is similar, but not equal, to the one used by Laskar[6]. The selected orbits have $\dot{z}_0$ between 0.24 and 0.92. Other values outside this interval lead to escape. The time span has been 1024 revolutions of the Moon. The Figure 6 shows the evolution of the four basic frequencies as a function of $\dot{z}_0$. In the figure the number of the orbit, k, is associated to $\dot{z}_0$ by $k = 50 \times \dot{z}_0$. The basic frequencies 1 to 4 correspond to the analogous of the long period frequency of the RTBP, the synodic Sun frequency, the short period and the vertical period, respectively. The solar frequency is constant, of course. It stops their appearition at orbit number 23 because the maximum amplitude (in any of the x, y or z coordinates) is less than 10^{-3}. Some remarks are relevant.

The long period frequency decreases (in absolute value) with the vertical amplitude. This is in good agreement with the RTBP behaviour, where a Normal Form computation around L_5 (see Gómez et al.[5]) gives, for the Earth-Moon problem, the expansion

$$\begin{aligned} \omega_l &= -0.298208 + 0.225319 I_v - 0.178982 I_v^2 + 0.071211 I_v^3 + 0.051720 I_v^4 + \\ &\quad + 0.000197 I_v^5 - 0.106373 I_v^6 + 0.045702 I_v^7 + \ldots, \end{aligned}$$

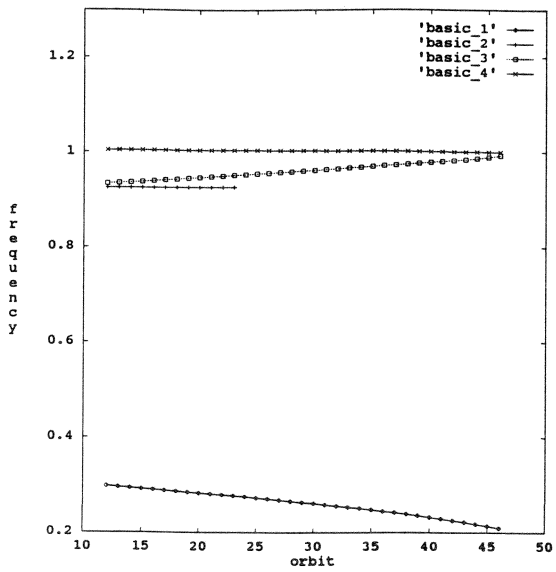

Figure 6. Evolution of the four basic frequencies along the family of orbits explored.

where the Hamiltonian is expanded in power series of three actions, I_s, I_l, I_v, associated to the short period, long period and vertical modes, respectively. The expansion above is just $\frac{\partial H}{\partial I_l}(0,0,I_v)$. For I_v one has $I_v = \frac{1}{2}(q_v^2 + p_v^2)$ (and similar for I_s, I_l) and q_v, p_v are rather close to z, $\dot{z}$. For completeness we give also ω_s and ω_v from the Normal Form of the RTBP as a function of the "vertical" action I_v (and $I_s = I_l = 0$):

$$\begin{aligned}
\omega_s &= 0.964501 + 0.089131 I_v - 0.055905 I_v^2 + 0.035475 I_v^3 - 0.004256 I_v^4 + \\
&\quad +0.042148 I_v^5 - 0.010521 I_v^6 + 0.048638 I_v^7 + \ldots, \\
\omega_v &= 1 - 0.004471 I_v - 0.000154 I_v^2 + 0.002088 I_v^3 + 0.000241 I_v^4 - 0.001846 I_v^5 \\
&\quad -0.000379 I_v^6 + 0.002006 I_v^7 + \ldots \ .
\end{aligned}$$

It follows that, in the RTBP and along the "vertical" family, the short period frequency increases and the vertical one decreases very slowly. This also happens in the bicircular model along the family used in the simulations, as can be checked in Figure 6. An important effect of the Sun is that it increases the value of the vertical frequency and decreases the short period frequency, with respect to what gives the RTBP. When the z-amplitude is of medium size (say, around $\dot{z}_0 = 0.22$, see next Section) there is a 1 to 1 resonance between the short period frequency and the solar one, leading to stability. On the other hand, when the z-amplitude increases (near $\dot{z}_0 = 0.93$) the vertical frequency and the short period one come into 1 to 1 resonance, leading again to instability. In this upper part the effect of the Sun (due to the variation of the frequencies with respect to the ones of the RTBP mentioned above) produces a delay in the instabilization. Indeed, in the RTBP the vertical family becomes unstable near $\dot{z}_0 = 0.89$.

As one can check with the expression of ω_v above, the dependence of ω_v with respect to I_v is quite mild. This also happens in the bicircular model. Vertically the motion is rather close to an harmonic oscillator. This can lead to a strong magnification of the effect of perturbations with frequencies close to resonance with the vertical one. The "twist condition" is very weak, say. The lack of robustness of the RTBP near L_4

and L_5 in front of the perturbations, for the Earth-Moon mass ratio, can also be seen from the torsion matrix (that is, the matrix of second derivatives of the Hamiltonian with respect to the actions). Using the Normal Form around L_5 one has that the torsion matrix is non definite and the torsion is small. The eigenvalues are 2.19621, -1.28718 and -0.02578, approximately.

Discussion and tentative explanations

We summarize first the results obtained so far. As presented in Gómez et al.[5], in the circular RTBP there is a big set of points which display stable motion around L_5. If, as we did, we take zero initial synodic velocity, this set of points is a kind of thick shell (which is close, but definitely departs, from part of a spherical surface). The form of this shell can be useful to try to derive "adapted" variables to carry out analytical studies. For the elliptic RTBP the results are not too far from the previous ones.

However the bicircular problem shows a quite different behaviour. Starting with zero initial velocity almost no point subsist until $z = 0.25$. But for z near 0.50 (i.e. orbits which start with zero velocity in synodical coordinates at a distance from the Earth-Moon plane which is of the order of magnitude of one half of the Earth-Moon distance) a big amount of points subsists. Near the periodic solution which replaces L_5 the behaviour is unstable. The fact that for higher values of z the motion seems to be on a 3-D torus which in turn is moving periodically with the period of the Sun, becomes more evident after a frequency analysis.

A part of the points which subsist in the bicircular problem do also subsist in the real one. A few points have been also seen to subsist starting on $z = 0$ in adimensional coordinates (see Gómez et al.[5]).

Now we present tentative explanations concerning the escape mechanism, the nature of the "boundary" of the set of remaining points and the rate of escape. These explanations are of different kind: geometrical and analytical.

Geometrical considerations. First we present these considerations for the RTBP. It seems that the local boundary of the stable set is related to resonances. May be these resonances are of high order (order= $\sum_{j=1}^{3} |k_j|$). Orders as 10, 12 or 17 are common in the Earth-Moon case. A complete description of the involved resonances is a hard task and it seems hopeless to try just analytical methods. A strong numerical effort is required to have a detailed description of those resonances.

Furthermore we have detected zones of stable motion which do not look as quasi-periodic, but chaotic close to resonance. This means that local resonance alone is not enough to produce escape. Let us try to explain this. The local resonance is due, in the simplest case to the appearition of some 2-D tori possessing stable and unstable manifolds. But to go out from the stable zone it is necessary that the stable manifold be connected to regions far away from L_5. These connections seem to be produced by a heteroclinic intersection with the stable manifold of some invariant object. Let us describe this object. We recall that the point L_3 is of saddle×centre×centre type. In particular it has a 4-D centre manifold. This manifold contains a Lyapunov orbit, halo orbits, etc. and also a Cantor set (with big fractal dimension) of 2-D tori in each level of energy. All these objects (periodic orbits and tori) are normally hyperbolic in their level of energy. It seems that the global stable manifold of this centre manifold ($W^s(W^c_{L_3})$), which is a manifold of codimension 1, acts as the effective boundary of the stable set.

Some numerical computations of intersections of this 5-D manifold with the set of the zero initial velocity, have been obtained. Generically this is a surface in the (x, y, z) variables. That surface can be plotted together with the set of stable points from direct numerical simulations (for instance using sections through z =ctant) to see if the suspected relation holds (see Gómez et al.[5]). For small values of μ the coincidence, between the 5-dimensional manifold and the boundary of the stable set, becomes more apparent.

Now we return to the bicircular model. We have already commented on the fact that the orbit which replaces the libration point has a hyperbolic behaviour in some directions. A transformation which (at least formally) skips the time dependence, if this is possible (see the third Section), produces an autonomous Hamiltonian with a fixed point of saddle × centre × centre type instead of the points L_4 or L_5. Hence, these fixed points also have codimension 1 invariant manifolds. We suspect that the "stability" domains are "confined" by the codimension 1 manifolds (of centre-stable and centre-unstable type) associated to the periodic (in the bicircular model) or quasiperiodic (in better models) orbits which take the place of L_3, L_4 and L_5.

We want to remark that these "rough boundaries" look very close to a "true" boundary when the mass parameter decreases (e.g., in the RTBP Sun-Jupiter case). Similar objects appear in many other problems when one looks at the stability zones around a general totally elliptic point (for instance, in symplectic maps in dimension four). In our case they come from the centre-unstable and centre-stable manifolds associated to the libration point L_3. In a similar way, the stability zones around the Moon, for instance, can be seen to have a rough boundary made of the centre-unstable and centre-stable manifolds associated to the libration points L_1 and L_2 of the Earth-Moon system. Some interesting transfers to halo orbits around the Moon or to highly elliptic lunar orbits, can use the fact that the manifolds for the L_1 Sun-Earth problem and the corresponding ones for the L_1 and L_2 Earth-Moon problems, do intersect for suitable epochs. But this topic is outside the scope of the present work.

Analytical considerations on the rate of escape. We shall consider the rate of escape of the points, according to the numerical simulations described before. It is readily seen that, for the bicircular model and the set of initial data we have taken, most of the points do not satisfy the stability criterion even after just 1 period of the Moon. We want to look at the ultimate rate of escape, after a transient (probably as long as a few hundreds of lunar periods, in our case).

First we look at a model problem. Consider the vicinity of a totally elliptic point of a Hamiltonian system and assume that the frequencies at that point satisfy a non-resonant diophantine condition (for some "admissible" resonances we refer to Giorgilli et al.[3]). Then the rate of diffusion of the points at a distance R of the fixed point is of the form $\exp(-\frac{c}{R^\alpha})$ (see Giorgilli et al.[3]) for some positive values of c and α, as it should be, in good agreement with the Nekhorosev[8] estimates. This is a bound on the time derivative of the radius, where the radius, R, is the square root of the sum of the actions (or of some positive definite linear combination of them). On the other hand we know that some power of the radius can be considered as a measure of the perturbation with respect to an integrable model, for instance, a Normal Form up to some degree. As it is well know, the set of points which are not in invariant tori is, in turn, a power of the perturbation parameter. Furthermore, we shall make the simplificative assumption that all the points which can go away from the fixed point, do really go away and with the maximum speed given by the previous bound on the speed of diffusion.

Summarizing, we consider, that for some radius, R_1, there are $R_1^s dR_1$ particles travelling away from 0 with a velocity equal to $\exp(-\frac{c}{R^\alpha})$, where s is some positive exponent. We consider that the particles escape from the neighbourhood of the elliptic point when they reach a value of the radius equal to R_0. Then it is possible to compute two values, $R_{1,n-1}$ and $R_{1,n}$ such that for R_1 between them, the escaping time is between $n-1$ and n. We define the set of points escaping in this time interval as e_n, and the set of points which remain at time n as r_n. Obviously $r_n = r_m - \sum_{j=m+1}^{n} e_j$ for $n > m$. After carrying out all the computations we obtain

$$r_n = L + \frac{A}{(\log n)^\beta},$$

where L (eventually zero) are the points which subsist for all time and A, β are positive quantities. Of course, β is related to the previous exponents α and s. We must remark that the formula above is a first approximation, more accurate formulas requiring corrections of the form $\log(\log n)$ to be added to the denominator. For moderate values of n this correction can be important. Furthermore, the "experimental" values of e_n, i.e., obtained from some numerical simulation, seem to behave in an irregular way. Hence, one has to consider successive values of r_{n_k} for $k = 1, 2, 3, \ldots$ not too close. To have values of n_k such that the fractions

$$\frac{r_{n_k} - r_{n_{k+1}}}{r_{n_{k-1}} - r_{n_k}}$$

have a limit different from 1, and has to take $n_{k+1} = n_k^\gamma$, for some γ greater than 1.

We have tested the approach above for the results of the numerical simulations, concerning the points which remain after n lunar revolutions in the bicircular model. To this end we have considered all the points which remain for more than 100 lunar revolutions (and up to 10000 revolutions due to the severe CPU time requirements). We have taken 64 time intervals, i.e., $n_0 = 100$ and $n_{64} = 10000$. Using the previous relation between successive values of n_k one has to take $\gamma = 1.010889$. Then we have obtained the best fit (by minimum squares, after taking logarithms in the formula above) for L, A and β by using the values of n with indices ranging from 32 to 64. The values obtained for the parameters are

$$L = 4636.3, A = 521306, \beta = 2.19437.$$

With those data the relative differences between the values given by the formula above and the observed data are less than 0.0022 for almost all the points (and certainly for the second half of the set of data), reaching 0.0211 for $n = 100$. We remark that, close to $n = 100$ the selected values of n are too close and the irregularity in the observed behaviour seems to give a good evidence that the initial transient should be considered till $n = 400$ or $n = 500$. The Figure 7 displays the data r_{n_k} for $k = 0, 1, \ldots, 64$ versus $\log(\log n)$ and the fit with the coefficients given above.

A natural question shows up. We have derived the formula for r_n, under some simplifying assumptions, for an elementary model. Why it seems to work in the present, harder case, of the bicircular model? An heuristic explanation can be as follows. The role played by the elliptic fixed point in the elementary model, is played by different invariant objects, mainly invariant tori. Instead of considering points in spherical shells which travel with some velocity, one has to consider subsets of toroidal annuli. The estimates for the speed of diffusion must also be of the Nekhorosev type, where now

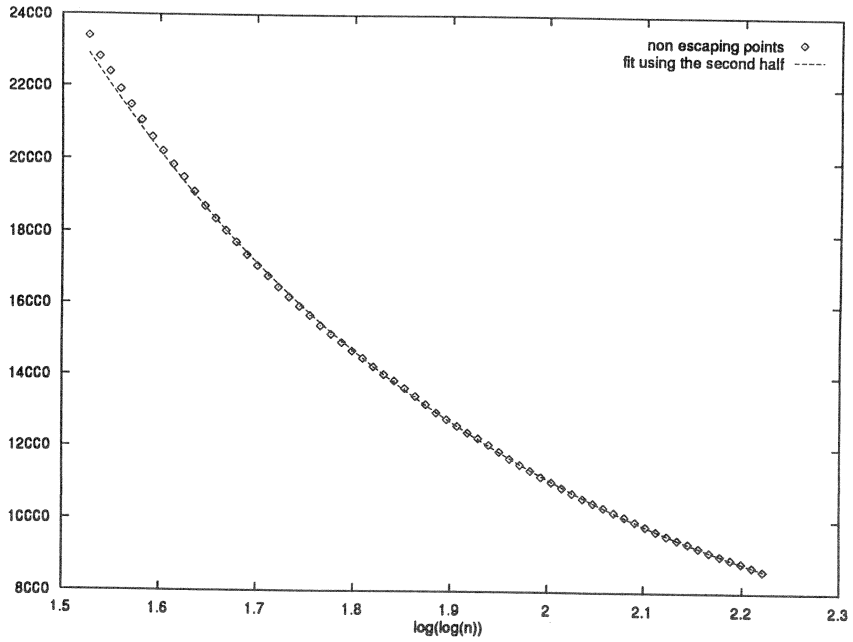

Figure 7

the meaning of R is the distance to some invariant object. Then one has to average to take into account different contributions, but if most of them are of the same kind, it is not a surprise that the general formula be of the same type as before.

SOME ANALYTIC COMPUTATIONS AND THE BOUNDARY OF INSTABILITY NEAR THE SMALL PERIODIC ORBIT

In this Section we shall consider different analytic tools to obtain an approximation of the boundary where the transition from instability to stability occurs in the bicircular model. We start at $z = 0$ near the small unstable periodic solution which replaces L_5, and then the vertical component is increased.

Normal Form

To obtain a Normal Form, suitable for the analysis in a vicinity of the small periodic orbit, first we introduce a new action variable, p_θ, canonically conjugate to the Sun's angle θ. Then the Hamiltonian becomes

$$H = \omega_S p_\theta + \frac{1}{2}(p_x^2 + p_y^2 + p_z^2) + y p_x - x p_y - \frac{1-\mu}{r_{PE}} - \frac{\mu}{r_{PM}} - \frac{m_S}{r_{PS}} - \frac{m_S}{a_S^2}(y \sin\theta - x \cos\theta),$$

without explicit appearition of the time. For shortness we just describe the steps to be carried out for the computation of the desired Normal Form, refering to Gómez et al.[5] for the details. We shall keep the names θ and p_θ for the Sun's angle and its related momentum through all the transformations. In fact θ remains unchanged, while p_θ changes because the initial Hamiltonian is not autonomous.

1. The first step is to shift the origin of coordinates to the periodic solution. One needs the Fourier expansion of the periodic orbit. This can be obtained by some symbolic computation or, in a more expeditive way, by computing both the periodic solution and the corresponding Fourier analysis numerically.

2. At this moment the Hamiltonian has no terms of first degree in the coordinates. All the other terms are monomials in the space coordinates and momenta, with coefficients depending periodically on θ. First we want to make the terms of degree 2 of the Hamiltonian, H_2, independent of θ. This is possible by Floquet's Theorem. Furthermore, it is easy to show that the transformation can be chosen to be canonical. One needs a representation of the (periodic) matrix of change of coordinates as a trigonometric series. Again one can use either a symbolic computation of the coefficients or a numerical Fourier analysis. In this way the actual terms of degree 2, H_2, (we keep H to denote the Hamiltonian in all the sequence of transformations) are independent of θ.

3. The next step is to put the terms of degree 2 in some suitable "diagonal" form:

$$H_2 = \lambda_1 Q_1 P_1 + \frac{1}{2}\omega_2(Q_2^2 + P_2^2) + \frac{1}{2}\omega_3(Q_3^2 + P_3^2),$$

where ω_2 and ω_3 are close to the frequencies of the RTBP ω_l and ω_v. The frequency ω_s is the one which has dissappeared. In its place the behaviour is hyperbolic with eigenvalue λ_1. We denote by Q_j and P_j for $j = 1, 2, 3$, the current variables.

4. For further use it is convenient to introduce complex coordinates by means of

$$X_j = \frac{Q_j + \sqrt{-1}P_j}{\sqrt{2}}, \qquad Y_j = \frac{\sqrt{-1}Q_j + P_j}{\sqrt{2}}, \qquad j = 2, 3,$$

and we put $X_1 = Q_1, Y_1 = P_1$. Then we have

$$H_2(X, Y) = \lambda_1 X_1 Y_1 + \sqrt{-1}\omega_2 X_2 Y_2 + \sqrt{-1}\omega_3 X_3 Y_3.$$

5. At this point we have to take the full Hamiltonian and perform all the changes described so far. To do this is quite convenient to put all the changes together. One obtains an affine transformation depending periodically on the angle θ. Then, as the inverses of the distances of the particle to Earth, Moon and Sun, r_{PE}, r_{PM} and r_{PS}, respectively, can be expanded by using the recurrence of the Legendre polynomials, it is easy to obtain the expansion of the Hamiltonian in the X_j and Y_j, $j = 1, 2, 3$ variables. The H_2 is already in Normal Form.

6. Now we have to show how to reduce the higher order terms of the Hamiltonian. The actual Hamiltonian is of the form

$$H(X, Y, \theta, p_\theta) = \omega_S p_\theta + H_2(X, Y) + \sum_{r>2} H_r(X, Y, \theta),$$

with H_2 as before and

$$H_r(X, Y, \theta) = \sum_{|k|=r} h_r^k(\theta) X^{k^1} Y^{k^2},$$

where $k = (k_1, \ldots, k_6)$, $k^1 = (k_1, k_2, k_3)$ and $k^2 = (k_4, k_5, k_6)$.

The purpose is to obtain a (periodic) change of variables transforming this Hamiltonian to a simpler one. That is, we will try to eliminate the dependence with respect to θ and, at the same time, to cancel the maximum possible number of monomials. Let us describe the method to be used. The main point is contained in the following proposition, which is presented in a general setting.

Proposition 1 *Let us consider the Hamiltonian*

$$H = \omega_S p_\theta + H_2(X,Y) + \sum_{i=3}^{r-1} H_i(X,Y) + H_r(X,Y,\theta) + H_{r+1}(X,Y,\theta) + \cdots,$$

where $r > 2$, $H_2(x,y) = \sum \omega_i X_i Y_i$ *(*$\omega_i \in \mathbb{C}$*),* $H_i(X,Y) = \sum_{|k|=i} h_i^k X^{k^1} Y^{k^2}$,

$H_r(X,Y,\theta) = \sum_{|k|=r} h_r^k(\theta) X^{k^1} Y^{k^2}$ *and* $h_r^k(\theta) = \sum_j h_{r,j}^k \exp(j\theta\sqrt{-1})$.

Let $G_r(X,Y,\theta) = \sum_{|k|=r} g_r^k(\theta) X^{k^1} Y^{k^2}$ *be a generating function defined as follows:*

(a) If $k^1 \neq k^2$ *then:*

$$g_r^k(\theta) = \frac{c_k - h_{r,0}^k}{<\omega, k^2 - k^1>} + \sum_{j\neq 0} \frac{h_{r,j}^k}{j\omega_S\sqrt{-1} - <\omega, k^2 - k^1>} \exp(j\theta\sqrt{-1}).$$

(b) If $k^1 = k^2$ *then:*

$$g_r^k(\theta) = \sum_{j\neq 0} \frac{h_{r,j}^k}{j\omega_S\sqrt{-1}} \exp(j\theta\sqrt{-1}).$$

Then, the new Hamiltonian, H', obtained from H by means of the change of variables given by the generating function G_r,

$$H' = H + \{H, G_r\} + \frac{1}{2!}\{\{H, G_r\}, G_r\} + \cdots,$$

satisfies that

$$H' = \omega_S p_\theta + H_2(x,y) + \sum_{i=3}^{r-1} H_i(x,y) + H'_r(x,y) + H'_{r+1}(x,y,\theta) + \cdots,$$

where $H'_r(x,y) = \sum (h')_r^k x^{k^1} y^{k^2}$,

$$(h')_r^k = \begin{cases} c_k & \text{if } k^1 \neq k^2 \\ h_{r,0}^k & \text{if } k^1 = k^2 \end{cases}$$

and x_j, y_j, $j = 1,2,3$ *denote the new variables after the change.*

We refer to Gómez et al.[5] for the proof.

Remark: The value c_k that appears in the function G_r is arbitrary. Usually it will be selected equal to zero, unless the divisors $<\omega, k^2 - k^1>$ were small, in which case it would be chosen equal to $h_{r,0}^k$. To have the final Hamiltonian as simple as possible, it would be desirable that all the c_k were chosen equal to 0 (except, of course, the ones corresponding to the resonant terms $k^1 = k^2$). But doing that, the expressions of the generating functions contain the divisors $<\omega, k^2 - k^1>$, that can be very small and produce convergence problems. For this reason, in practice, one can use a threshold ε and select $c_k = 0$ only when the corresponding divisor is greater than ε. Otherwise it is chosen to be equal to $h_{r,0}^k$. With this, one can expect to obtain a final Hamiltonian with only a few monomials, being a useful approximation over a relevant region of the phase space.

The results of the computation of the Normal Form

The steps described above have been implemented and applied to the case of the bicircular model. The computations have been done, in fact, for the periodic orbit replacing L_4. They are similar for L_5. Using a threshold $\varepsilon = 10^{-2}$ for the small divisors, we have computed the Normal Form up to degree 12 (in the cartesian coordinates, and, hence, up to degree 6 in the actions). This expansion contains only the exactly resonant terms (this is because there is not any small divisor less than 10^{-2} up to order 12), and this implies that the Normal Form is integrable.

For the analysis it is convenient to translate the final Hamiltonian to real coordinates (we are interested on the behaviour of the system for real values of the coordinates). We use the inverse of the change of variables used when complexifying:

$$u_i = \frac{x_i - \sqrt{-1}y_i}{\sqrt{2}}, \quad v_i = \frac{-\sqrt{-1}x_i + y_i}{\sqrt{2}}, \quad i = 2, 3,$$

and (as before) $u_1 = x_1$ and $v_1 = y_1$.

We can write this Hamiltonian in an simpler form by defining the actions

$$I_1 = u_1 v_1, \quad I_2 = \frac{1}{2}(u_2^2 + v_2^2), \quad I_3 = \frac{1}{2}(u_3^2 + v_3^2).$$

We note that the variables u_3 and v_3 are rather close to z and $\dot{z}$.

We give that Hamiltonian in Table 2, where the three first columns contain the exponents of I_1, I_2 and I_3, and the fourth one contains the corresponding coefficient.

The Normal Form obtained so far shows that, around the equilibrium point which takes the place of the periodic orbit, the Hamiltonian behaves like a saddle $\times$ centre $\times$ centre. The action variable I_1 is related to the saddle. The local formal centre manifold is defined by $I_1 = 0$. For any couple of (small enough) positive values of I_2 and I_3, we obtain an approximation of a 2-D torus, the frequencies being similar to the long period one and the vertical one of the RTBP. Going back through the changes of variables, we obtain 3-D tori, the new frequency being the solar synodic one. Along the full centre manifold we can compute the normal hyperbolicity. This is given by the function $\lambda = \frac{\partial H}{\partial I_1}(0, I_2, I_3)$. Of course, at the origin λ is the coefficient of I_1, that is, λ_1.

We can consider the part of the centre manifold restricted to $I_2 = 0$ having I_3 as unique parameter. This describes a family of unstable periodic orbits of the Normal Form, corresponding to 2-D tori of the bicircular problem. We want to know the value of I_3 for which the stability changes (and so does the dimension of the centre manifold). From Table 2 we obtain the following expression for λ, now being simply $\lambda(I_3)$:

$$\begin{aligned}\lambda(I_3) \;=\; & -0.013852 + 0.257784 I_3 + 2.607311 I_3^2 + 50.49658 I_3^3 + \\ & + 1299.415 I_3^4 + 38773.19 I_3^5 + \dots \ .\end{aligned}$$

Of course, the Normal Form of the kind considered here can not be convergent when the desired bifurcation occurs (letting aside the small divisors problems that, in fact, prevent from convergence in any open set). We can set $\lambda(I_3) = 0$ with the expression given here to obtain a critical value of I_3. We find $I_3 = 0.030481$. This gives a value for, say v_3 if $u_3 = 0$, of 0.246905. The observation concerning u_3 and v_3 tells us that this gives an idea of the suitable value of $\dot{z}$ if $z = 0$. One can try to improve a little bit

Table 2. Hamiltonian in Normal Form around the small unstable periodic orbit of the bicircular problem.

1	0	0	-.1385220057080626D-01	2	1	2	-.1864225143531067D+07
0	1	0	-.3005039252506557D+00	2	0	3	.5304991639454239D+05
0	0	1	.1004006523604956D+01	1	4	0	-.4052415718452325D+08
2	0	0	.8515077021376744D+00	1	3	1	-.1360849493836872D+08
1	1	0	-.3324999040181953D+01	1	2	2	.5520658628803922D+05
1	0	1	.2577837871812799D+00	1	1	3	-.5699313229911387D+05
0	2	0	.3270045540584760D+00	1	0	4	.1299414585487088D+04
0	1	1	.2307565086566667D+00	0	5	0	-.2448924023843400D+07
0	0	2	-.4032569929542033D-02	0	4	1	.1501613346456005D+07
3	0	0	.1037922842258645D+03	0	3	2	.1711773835404635D+06
2	1	0	-.4565506222871429D+03	0	2	3	.1632111440703841D+04
2	0	1	.3321899325302790D+02	0	1	4	-.9347880155609670D+02
1	2	0	-.2146275456385827D+04	0	0	5	.1551444240916563D+01
1	1	1	-.4784863921619558D+02	6	0	0	.2987999377729337D+10
1	0	2	.2607311336225566D+01	5	1	0	-.2411838508681229D+11
0	3	0	.3096780901433248D+02	5	0	1	.1782373214959049D+10
0	2	1	.2494045964589006D+01	4	2	0	-.8672410442035261D+12
0	1	2	-.2270782098281886D+00	4	1	1	-.1052914435151395D+11
0	0	3	.9052424722400662D-03	4	0	2	.4078275712719006D+09
4	0	0	.2499474130723898D+05	3	3	0	-.1116963084432885D+12
3	1	0	-.1379292451759401D+06	3	2	1	-.2505479615606837D+11
3	0	1	.1018100448948390D+05	3	1	2	-.1622067585088890D+10
2	2	0	-.1748183316981774D+07	3	0	3	.4405125443309778D+08
2	1	1	-.3120287556473054D+05	2	4	0	.1858745324134717D+13
2	0	2	.1318002728888036D+04	2	3	1	.5250659284283364D+11
1	3	0	.1288209631845397D+07	2	2	2	.4716462061283490D+09
1	2	1	.4931293498255790D+05	2	1	3	-.1020454848295031D+09
1	1	2	-.1616391528463035D+04	2	0	4	.2189796196165091D+07
1	0	3	.5049658419448990D+02	1	5	0	-.4715529712174978D+12
0	4	0	-.2709111320415782D+05	1	4	1	-.2821114699272034D+11
0	3	1	-.3353580692587518D+04	1	3	2	.9001096107686855D+09
0	2	2	.6040532947455749D+01	1	2	3	.8144952535614336D+07
0	1	3	-.1944360487197618D+01	1	1	4	-.2160288537221536D+07
0	0	4	.4157193549100161D-01	1	0	5	.3877318738835637D+05
5	0	0	.7974901100840953D+07	0	6	0	.8912688288853617D+10
4	1	0	-.5407213341839783D+08	0	5	1	.5578588877780112D+09
4	0	1	.3996634109602074D+07	0	4	2	-.1075748940803764D+09
3	2	0	-.1253144279500538D+10	0	3	3	-.3296022936390645D+07
3	1	1	-.1807321686550926D+08	0	2	4	.8616212602968118D+05
3	0	2	.7164000260814325D+06	0	1	5	-.4191316945624839D+04
2	3	0	.8247843021482749D+09	0	0	6	.5876577678574162D+02
2	2	1	.1380185818563243D+08				

the estimate by proceding in an heuristic way. In the formula for $\lambda(I_3)$ one can assume that the coefficients of higher order increase at a given rate, similar or slightly higher than the quotient of the coefficients of degree 5 and 4. Assuming an increase by a factor 30 one gets a critical value for $\dot{z}$ of 0.233358, and if the factor is 40, one obtains 0.217431. However, one can not rely very much on this result, the main problem being the low order at which we have computed the Normal Form. To increase the order in a substantial way seems to be a formidable task. We better proceed to produce estimates using a different analytic approach, which can lead to a higher order expansion with a similar computational effort.

The equations and the algorithm for the computation of unstable 2-D tori

Vertical periodic orbits of the circular 3-D RTBP give rise, in the case of the bicircular problem, to 2-D tori. One of the frequencies is the vertical one, the other being the solar synodic frequency. The Normal Form procedure gives good results only for small z amplitude. We proceed to the direct computation of these tori.

Let ξ, η, ζ be the coordinates with respect to the L_5 point in the synodic system (for the L_4 case is similar). Then the equations of motion are ($'= d/dt$)

$$\begin{aligned} \xi'' &= 2\eta' + \frac{3}{4}\xi - a\eta + \frac{\partial}{\partial \xi}V, \\ \eta'' &= -2\xi' - a\xi + \frac{9}{4}\eta + \frac{\partial}{\partial \eta}V, \\ \zeta'' &= -\zeta + \frac{\partial}{\partial \zeta}V, \end{aligned}$$

where $a = (\sqrt{27}/4)(1-2\mu)$ and V is the potential accounting for the higher order terms of the RTBP plus the solar effect:

$$\begin{aligned} V &= (1-\mu)\sum_{n\geq 3} P_n\left(\frac{(1/2)\xi - (\sqrt{3}/2)\eta}{\rho}\right)\rho^n + \mu\sum_{n\geq 3} P_n\left(\frac{-(1/2)\xi - (\sqrt{3}/2)\eta}{\rho}\right)\rho^n \\ &\quad + \frac{m_S}{a_S}\sum_{n\geq 2} P_n\left(\frac{(\xi+\mu-1/2)\cos(\omega_S t) - (\eta+\sqrt{3}/2)\sin(\omega_S t)}{R}\right)\frac{R^n}{a_S^n}. \end{aligned}$$

In the last expression one has $\rho^2 = \xi^2+\eta^2+\zeta^2$, $R^2 = (\xi+\mu-1/2)^2+(\eta+\sqrt{3}/2)^2+\zeta^2$, and a_S, m_S, ω_S denote the radius of the orbit, the mass and frequency of the Sun.

We write first $\xi = \xi_0 + \overline{\xi}$, $\eta = \eta_0 + \overline{\eta}$, $\zeta = \zeta_0 + \overline{\zeta}$, where ξ_0, η_0 ($\zeta_0 = 0$) are the coordinates of the periodic solution, with frequency ω_S, which replaces L_5 in the bicircular problem. Let $\psi = \exp(i\omega_S t)$. Then $\xi_0 = \sum_k \xi_{00k}\psi^k$, $\eta_0 = \sum_k \eta_{00k}\psi^k$. The coefficients are known from the numerical solution and numerical Fourier analysis. We look for a solution of the form (with complex coefficients)

$$\xi = \sum_{l,j,k} \xi_{ljk}\alpha^l\phi^j\psi^k, \eta = \sum_{l,j,k} \eta_{ljk}\alpha^l\phi^j\psi^k, \zeta = \sum_{l,j,k} \zeta_{ljk}\alpha^l\phi^j\psi^k,$$

with $l \geq 0$, $j,k \in Z$, where $\phi = \exp(i\omega t)$, α is some (vertical) amplitude, which is being considered as a parameter, and ω is an amplitude depending (vertical) frequency, of the form $\omega = \omega_0 + \omega_2\alpha^2 + \omega_4\alpha^4 + \ldots$. As normalizing condition on α we choose $\zeta_{1,1,0} = 1/2$, $\zeta_{l,1,0} = 0$, $\forall l > 1$. As the solutions are real we have $\xi_{l,j,k} = \overline{\xi}_{l,-j,-k}$ and similar relations hold for the η and ζ coefficients. Furthermore, the symmetries of the problem imply that in ξ, η, the indices l and j are even, in the ζ they are odd, and in all the cases $|j| \leq l$.

Let us denote by ξ_l the sum $\sum_{j,k} \xi_{ljk}\phi^j\psi^k$. So $\overline{\xi} = \alpha\xi_1 + \alpha^2\xi_2 + \ldots$. Similar representations are used for $\overline{\eta}$, $\overline{\zeta}$. First we discuss how we have computed the terms in ζ_1 (ξ_1 and η_1 being zero) and then how to proceed, in a different way, to compute ξ_n, η_n, ζ_n, $n \geq 2$.

The standing equation is $\zeta'' = -\zeta + (\partial/\partial\zeta)V$, and this, to order 1 in α, reads $\zeta_1'' = -\zeta_1 + \frac{\partial^2}{\partial\zeta^2}V(\xi_0, \eta_0, 0)\zeta_1$. Furthermore we keep $\zeta_{110} = 1/2$, and we have to determine ω_0, where $(\zeta_{1jk}\phi^j\psi^k)'' = \zeta_{1jk}\phi^j\psi^k[-(j\omega_0 + k\omega_S)^2]$. By equating terms in $\phi^j\psi^k$ in the

previous equation for ζ_1 we get a linear system (but the problem is nonlinear because of ω_0) in the ζ_{1jk} coefficients $|j| \leq j_{max}$, $0 \leq k \leq k_{max}$. As the system is homogeneous one has to take the right value of ω_0 to make the solution possible and some normalization, as it has been said. There are several possible ways to solve the problem. We can get ω_0 from the numerical integration of the variational equations along the periodic solution $(\xi_0, \eta_0, 0)$. Another possibility is to use an iterative process.

We write $(\zeta_1'' + \zeta_1)^{(k+1)} = \frac{\partial^2}{\partial \zeta^2} V(\xi_0, \eta_0, 0)(\zeta_1)^{(k)}$ and we start with the initial guess $\zeta_1^0 = (1/2)\phi$ (notice that we had to add to the representation used the complex conjugate and that if $k = 0$ then the range of j in the representation is $0 \leq j \leq j_{max}$). Let us denote by $c_1^{(k)}(\phi, \psi)$ the product $\frac{\partial^2}{\partial \zeta^2} V(\xi_0, \eta_0, 0)(\zeta_1)^{(k)}$. As we want to keep $\zeta_{1,1,0} = 1/2$ this gives immediately the value of $\omega_0^{(k+1)}$ by equating the terms in $\phi^1\psi^0$: $[1 - (\omega_0^{(k+1)})^2](1/2) = c_{1,1,0}^{(k)}$. Then the terms $\zeta_{1,j,k}^{(k+1)}$, $(j,k) \neq (1,0)$ are given by $\zeta_{1,j,k}^{(k+1)} = c_{1,j,k}^{(k)}/(1 - (j\omega_0^{(k+1)} + k\omega_S)^2)$. When $\zeta^{(k+1)}$ is available we substitute to get the new $c_1^{(k+1)}$ and the process is repeated.

Unfortunately, that process, as it is described, fails to converge. However, it has been seen that it has just one unstable direction. This suggests to use an extrapolation method (Aitken) that then leads to convergence. The value obtained for ω_0 is 1.0040065236..., in perfect agreement with the monodromy matrix.

When ζ_1 is available we could continue the iterative- extrapolation process. However the number of unstable directions increases when we look for (ξ_n, η_n, ζ_n) (remark that if n is even we had to solve only for (ξ_n, η_n) and if n is odd, only for ζ_n). Hence we need a different method. We describe first the procedure for (ξ_n, η_n).

We write the equations as

$$\xi_n'' - 2\eta_n' - \left(\frac{3}{4}\xi_n - a\eta_n + \frac{\partial^2 V}{\partial \xi^2}(\xi_0, \eta_0, 0)\xi_n + \frac{\partial^2 V}{\partial \xi \partial \eta}(\xi_0, \eta_0, 0)\eta_n\right) =$$

$$= \left[\frac{\partial V}{\partial \xi}(\overline{\xi}_{n-1}, \overline{\eta}_{n-1}, \overline{\zeta}_{n-1}) - \overline{\xi}_{n-1}'' + 2\overline{\eta}_{n-1}'\right]\Big|_n ,$$

$$\eta_n'' + 2\xi_n' - \left(a\xi_n + \frac{9}{4}\eta_n + \frac{\partial^2 V}{\partial \xi \partial \eta}(\xi_0, \eta_0, 0)\xi_n + \frac{\partial^2 V}{\partial \xi^2}(\xi_0, \eta_0, 0)\eta_n\right) =$$

$$= \left[\frac{\partial V}{\partial \eta}(\overline{\xi}_{n-1}, \overline{\eta}_{n-1}, \overline{\zeta}_{n-1}) - \overline{\eta}_{n-1}'' - 2\overline{\xi}_{n-1}'\right]\Big|_n ,$$

where the notation $\overline{\xi}_{n-1}$ means $\xi_0 + \alpha\xi_1 + \ldots \alpha^{n-1}\xi_{n-1}$ (and similar for η, ζ) and $[\ ]|_n$ denotes the terms in α^n. Notice that in the $[\ ]|_n$ terms, there is a contribution in α^n when ξ, η, ζ are known to order $n-1$ in α because of the nonlinearities in the derivatives of V and because of the powers of α appearing in ω in the time derivatives.

For ζ_n (n odd) the procedure is similar, but keeping $\xi_{n,1,0} = 0$ allows the determination of ω_{n-1} when equating the terms in $\alpha^n\phi^1\psi^0$.

We remark that the systems of linear equations which appear to get (ξ_n, η_n) for $n = 2, 4, \ldots$ have the same matrix. The same thing happens for ζ_n, $n = 3, 5, \ldots$. Furthermore the systems for different values of j are uncoupled. Some caution has to be taken with the poorly conditioned character of the matrices, specially in the ζ_n case, $j = 1$. It has been found very useful, to decrease the numerical errors, to work in quadruple precision complex variables (or simulate it, depending on the software). The computation of the derivatives of V is shortened by the use of recurrences derived from the ones of Legendre polynomials.

Truncated power series results

The previous algorithm has been implemented with l_{max} (and hence, j_{max}) = 41 and k_{max} = 18. From the results of the second Section, we know that the previous 2-D unstable tori should be convergent up to moderate values of α (and, definitely, less than 0.25). In fact, the coefficients of ω seem to give a radius of convergence ($\lim_{n\to\infty, n\ even} \omega_n^{-1/n}$) close to 0.219. If, instead, we consider the norm of ξ_n as $|\xi_n| = \sum_{j,k} |\xi_{n,j,k}|$, we can also get an idea of the radius of convergence of the expansions with respect to α. The same is true for the $|\eta_n|$, $|\zeta_n|$. All of them give essentially the same radius of convergence as ω. Notice that for n large the numerical errors propagated by the successive solutions at the previous orders, start to show up, giving a slightly irregular behavior of the components (see Table 3).

A test has been passed as follows. Consider a value of α and look at the approximate quasiperiodic solution provided by the formulas above. For a given value of t one can compute $\xi, \eta, \zeta, \xi', \eta', \zeta', \xi'', \eta'', \zeta''$. Then, from the positions and velocities, one obtains the acceleration from the direct equations of motion for the bicircular problem. The difference with respect to the values computed from the series is the residual acceleration. Table 4 shows some results for a time span of 100 adimensional units with time step 0.1. There is a remarkable agreement till $\alpha = 0.16$ and still acceptable till $\alpha = 0.2$. Figures 8 and 9 show the (x, z) and (x, y) projections of the analytic orbits computed for $\alpha = 0.10$ and $\alpha = 0.18$. In both Figures we plot just one dot for each value of t, these values being of the form $k \times 0.1$ for $k = 0, 1, \ldots, 100000$, without joining successive points in the orbit. One can suspect that in the case of Figure 9 we are close to a resonance. The frequencies turn out to be $\omega_S = 0.9251959855$ and $\omega_v = 1.0038778841$, not too close to produce a low order resonance. The behaviour seen in the Figure 9 is due to the time interval. Indeed, $18 \times \omega_S \times 0.1 + 46 \times \omega_v \times 0.1 - 2\pi$ is less than 3×10^{-6}. Taking 1.1×10^6 points (with the same time step) shows a very good equidistribution of points.

Discussion and Conclusions

Invariant 2-D unstable tori have been found by a symbolic manipulation implementation of a version of the Lindstedt-Poincaré method. By a suitable modification and an additional computational effort, one can compute also 3-D unstable tori. The frequency to be added is equivalent to the long period frequency of the RTBP. We also recall that the action of the Sun produces an increase of the vertical frequency (whose limit is 1 in the RTBP when the vertical amplitudes goes to zero). However, the behaviour of the "vertical" frequency when the amplitude increases is preserved. An increase of the amplitude produces a reduction of the frequency. The boundary of convergence is associated to a bifurcation (as was already outlined in the previous Section): The tori lose their hyperbolic character, becoming stable (in some weak sense). They can be considered as "big" KAM tori of the bicircular problem. As sketched in the second Section, the lose of stability, for z amplitudes around 0.22, is due to a resonance between the "short period frequency" and the solar one.

The existence of stable zones for the bicircular model (and, in fact for the real model, this one being a slight perturbation of the previous one, in the region of the study) opens the way to a new series of space missions. Indeed, the stability of the orbits implies that no station keeping is needed for the orbit dynamics. Furthermore is has been seen that it is relatively cheap to reach those zones from a GTO or a parking

Table 3. For the variables ω, ξ, η and ζ the non zero norms of the coefficients for orders of α from 16 up to 41 are given, and also the estimated radii of convergence.

	ω			ξ	
16	.125580D+06	.214260D+00	16	.650326D+08	.226198D+00
18	.270934D+07	.215292D+00	18	.127693D+10	.225673D+00
20	.580404D+08	.216056D+00	20	.251957D+11	.225123D+00
22	.123691D+10	.216618D+00	22	.499663D+12	.224556D+00
24	.262616D+11	.217024D+00	24	.996014D+13	.223978D+00
26	.556124D+12	.217307D+00	26	.199577D+15	.223396D+00
28	.117566D+14	.217492D+00	28	.401983D+16	.222818D+00
30	.248292D+15	.217600D+00	30	.813808D+17	.222250D+00
32	.524165D+16	.217644D+00	32	.165577D+19	.221697D+00
34	.110661D+18	.217639D+00	34	.338509D+20	.221164D+00
36	.233726D+19	.217592D+00	36	.695257D+21	.220654D+00
38	.494006D+20	.217514D+00	38	.143426D+23	.220170D+00
40	.104511D+22	.217412D+00	40	.297108D+24	.219713D+00
	η			ζ	
16	.471914D+08	.226247D+00	17	.547271D+08	.226223D+00
18	.926194D+09	.225725D+00	19	.107433D+10	.225699D+00
20	.182662D+11	.225178D+00	21	.211934D+11	.225148D+00
22	.362062D+12	.224612D+00	23	.420179D+12	.224586D+00
24	.721361D+13	.224034D+00	25	.837397D+13	.224001D+00
26	.144470D+15	.223453D+00	27	.167751D+15	.223425D+00
28	.290843D+16	.222874D+00	29	.337852D+16	.222828D+00
30	.588521D+17	.222304D+00	31	.683700D+17	.222295D+00
32	.119684D+19	.221749D+00	33	.139109D+19	.221694D+00
34	.244575D+20	.221213D+00	35	.284283D+20	.221208D+00
36	.502114D+21	.220701D+00	37	.583760D+21	.220677D+00
38	.103540D+23	.220214D+00	39	.120527D+23	.220077D+00
40	.214405D+24	.219754D+00	41	.249632D+24	.219731D+00

Table 4. Test of errors for the unstable 2-tori obtained by the Lindstedt-Poincaré method. The first column gives the amplitude. 1he other three columns give the residual accelerations in x, y and z, respectively.

.11	.118048D−13	.124831D−13	.181799D−14
.12	.152708D−13	.175892D−13	.262290D−14
.13	.148928D−12	.204631D−12	.291295D−13
.14	.337156D−11	.490744D−11	.710931D−12
.15	.669266D−10	.957271D−10	.148328D−10
.16	.112226D−08	.156734D−08	.259666D−09
.17	.162949D−07	.221698D−07	.391360D−08
.18	.210096D−06	.277842D−06	.532121D−07
.19	.246850D−05	.319889D−05	.660951D−06
.20	.272526D−04	.352209D−04	.769544D−05
.21	.292881D−03	.380884D−03	.873664D−04

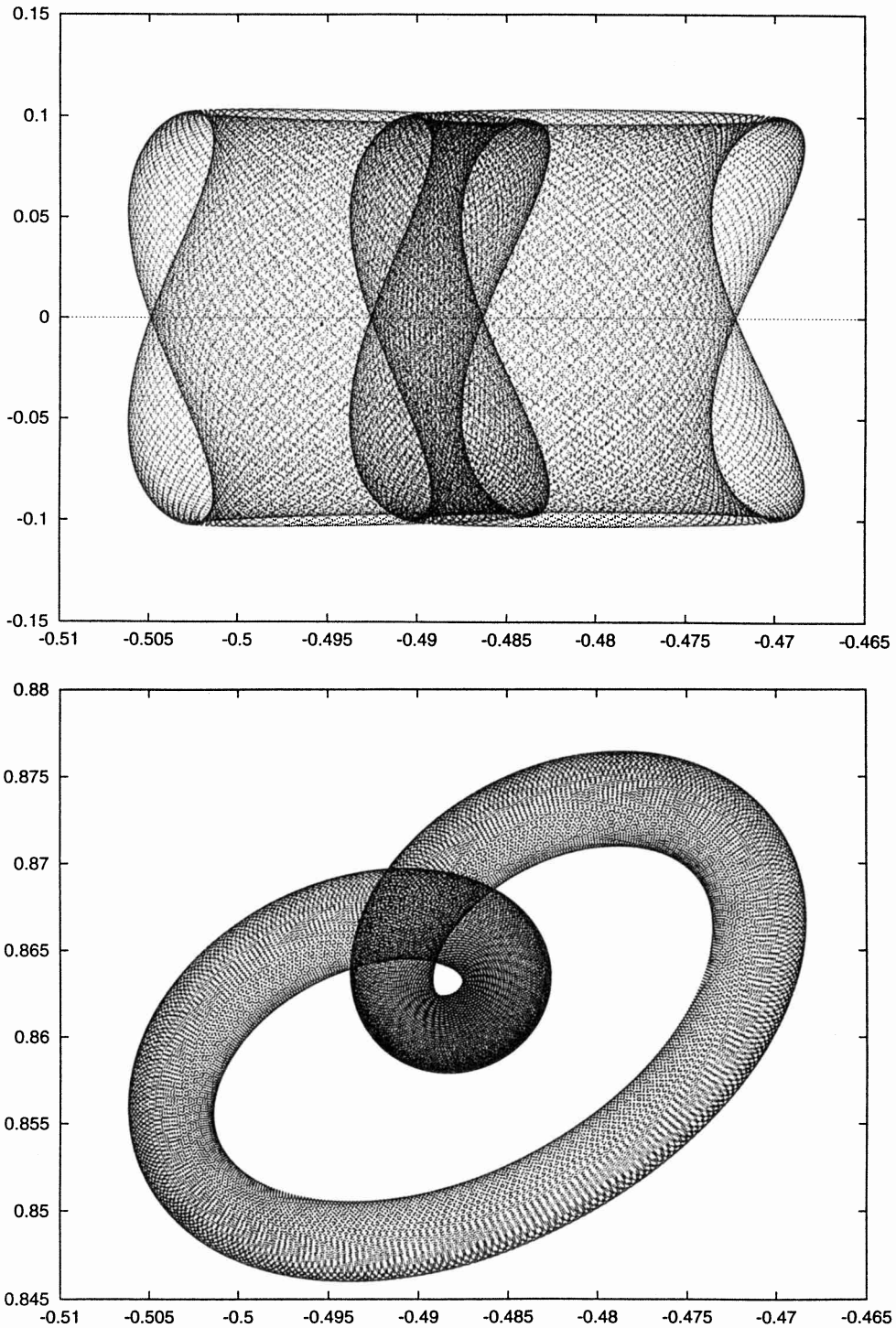

Figure 8. Projections (x, z) (top) and (x, y) (bottom) of the 2-torus of z amplitude equal to 0.10. The final time is 10000 units (recall 2π is equivalent to the lunar period). The time step is 0.1 time units. The distance unit is the Earth-Moon distance.

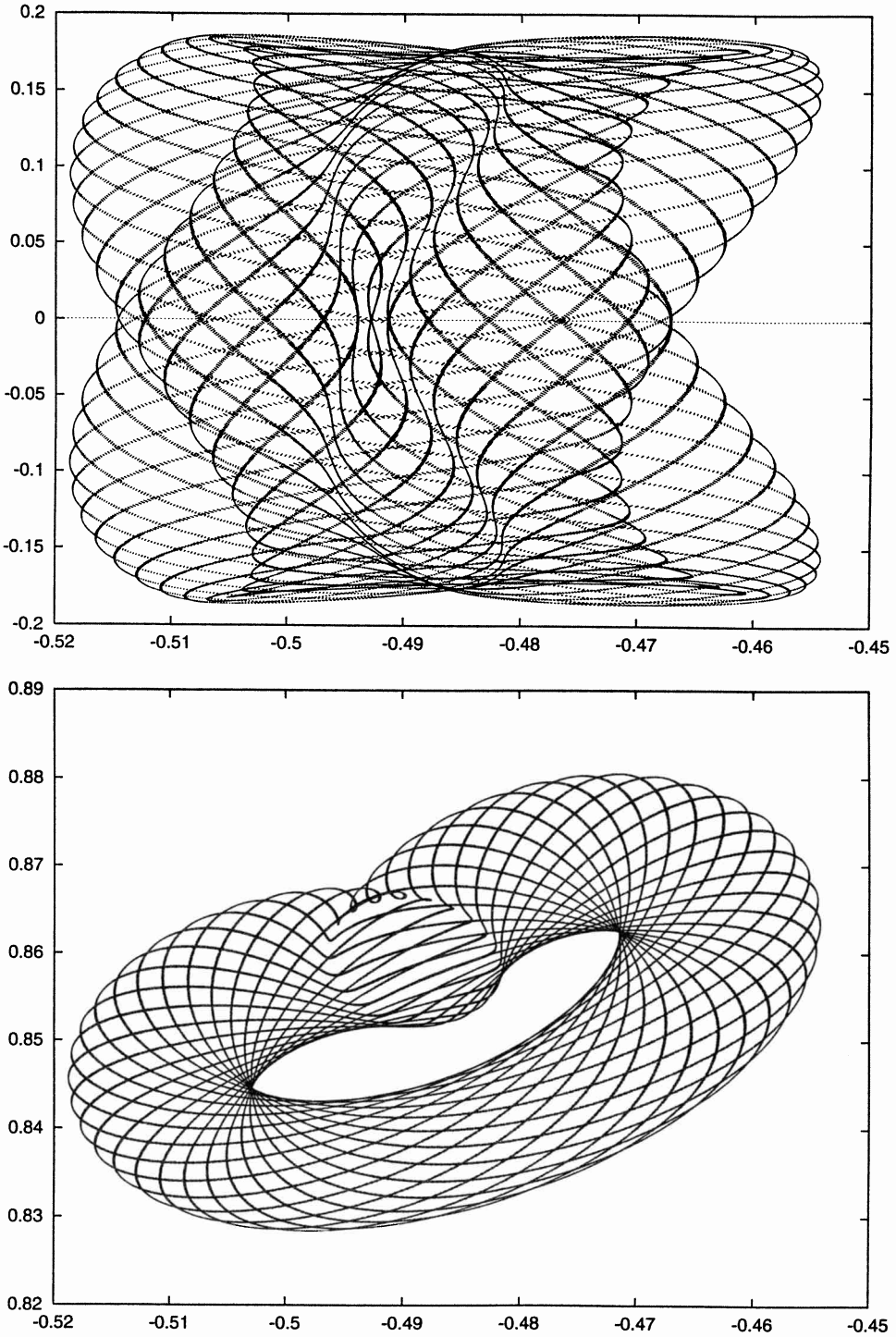

Figure 9. Projections (x, z) (top) and (x, y) (bottom) of the 2-torus of z amplitude equal to 0.18. The final time is 10000 units. All the units as in the previous Figure.

orbit around the Earth (see Gómez et al.[5]). Possible space missions using this kind of orbits are: Parking orbits for micro spacecrafts, ready to travel to asteroids approaching the Earth-Moon system (possibly with a lunar gravity assisted manoeuvre); Deep space astronomy, close enough to the Earth to realize easely the observational commands, and far enough to have low noise level.

Acknowledgements

The authors have been supported by a CICYT Grant ESP91-0403 from the Spanish Ministery of Education. They are indebted to the staff of ESOC, specially to Dr. J. Rodríguez Canabal, for his encouragement during the realization of the ESOC Contract 9711/91/D/IM(SC), where applications of the present work can be found in detail.

REFERENCES

1. V.I. Arnol'd and A. Avez. "Problèmes Ergodiques de la Mécanique Classique," Gauthier-Villars, Paris (1967).

2. E. Fontich and C. Simó,The splitting of separatrices for analytic diffeomorphisms, *Ergodic Theory and Dynamical Systems* **10**, 295-318 (1990).

3. A. Giorgilli, A. Delshams, E. Fontich, L. Galgani and C. Simó, Effective stability for a Hamiltonian system near an elliptic equilibrium point, with an application to the restricted three body problem, *J. Differential Equations* **77**, 167-198 (1989).

4. G. Gómez, J. Llibre, R. Martínez and C. Simó. "Study on Orbits near the Triangular Libration Points in the Perturbed Restricted Three Body Problem," ESOC Contract 6139/84/D/JS(SC), Final Report (1987).

5. G. Gómez, A. Jorba, J. Masdemont and C. Simó. "Study of Poincaré Maps for Orbits near Lagrangian Points," ESOC Contract 9711/91/D/IM(SC), Final Report (1993).

6. J. Laskar, A numerical experiment on the chaotic behaviour of the solar system, *Nature* **338**, 237-238 (1989).

7. V.F. Lazutkin, I.G. Schachmanski and M.B. Tabanov, Splitting of separatrices for standard and semistandard mappings, *Physica* **D40**, 235-248 (1989).

8. N.N. Nekhoroshev, An exponential estimate of the time of stability of nearly-integrable Hamiltonian systems, *Russ. Math. Surveys* **32**, No 6, 1-65 (1977).

9. C. Simó, Averaging under fast quasiperiodic forcing, University of Barcelona Preprint (1993).